

### 3.2.6 M13 configurations

Alignment and calibration runs used different M13 settings. For example, drift chamber alignment used higher momentum pions, and calibration of the time expansion chambers used a spread muon beam. An entire data set was taken at a lower momentum of 28.9 MeV/ $c$  as a consistency check. The special configurations and sets are described in more detail in Section 8.4.

## 3.3 Measuring the muon beam

The final polarisation of the muons must be known with high precision. Ideally this would be measured using the velocity vector inside the detector. However, this would be technically challenging since the detector is within a 2 T magnetic field (see Section 3.7). Instead the muon beam is measured at the end of the M13 channel, before the muons have encountered significant material or magnetic field. At this point, the muon beam has encountered a small amount of material, so that a muon's momentum and spin vectors are opposite to an acceptable approximation. The muons can then be simulated to determine their final polarisation.

In 2002, measurements of the muon beam were made using a wire chamber. Other experiments have simply used a scintillator[15]. However, the systematic uncertainty goal for  $P_{\mu}^{\pi} \xi$  meant that a more precise method was needed. Prior to accumulating data in 2004, a pair of identical time expansion chambers<sup>14</sup> were constructed to measure individual muon trajectories with high precision. These chambers started to be used in 2004, when the experiment's original  $P_{\mu}^{\pi} \xi$  measurement was carried out. The first time expansion chamber (TEC) module measured  $x$  and  $\theta_x$ , and the second module measured  $y$  and  $\theta_y$ . In order to minimise multiple scattering while measuring the trajectory, the mass of the system was kept as low as possible. Despite these efforts, the multiple scattering of the TECs meant they could not remain in place during nominal data acquisition. Therefore the modules were inserted on a weekly basis for approximately an hour of beam measurements. The alignment and calibration of the TEC modules is described in Sections 3.14 and 3.16. The analysis of the data from the TECs is detailed in Chapter 5.

The positioning of the box containing the modules is shown in Fig. 3.5. The TEC modules are located close to the F3 focus, where the beam has a small extent. When the muon beam

---

<sup>14</sup>A time expansion chamber is a type of time projection chamber. The drift volume is divided into a low electric field region separated from a higher field amplification region. The result is a higher precision measurement.

encounters the TECs, it has passed through no material except for a single thin ( $6\ \mu\text{m}$  Mylar) beam line window. The low magnetic field means that trajectories are well approximated by straight lines, which simplifies the analysis.

The TEC modules are labelled “X Module” and “Y Module” in Fig. 3.6. Each module is  $8.0\ \text{cm}$  long with an active area of  $6.0\ \text{cm} \times 6.0\ \text{cm}$ . They are inside a box that is filled with low pressure ( $8\ \text{kPa}$ ) Dimethylether<sup>15</sup> gas that constantly flows at a rate of  $100\ \text{cm}^3/\text{min}$ . An electric field is maintained over the drift volume by a graded voltage applied to drift wires, as shown in Fig. 3.7. Charged particles ionise the gas, and this ionisation drifts towards the sense plane. The electrons enter a high field region, separated by grid (“guard”) wires. In the high field “multiplication region” the electrons are accelerated towards small diameter ( $25\ \mu\text{m}$ ) sense wires where they avalanche and cause a signal. The time of signal relative to the muon trigger is then converted into a distance using space-time relationships (STRs). Each TEC had 24 sense wires at  $0.2\ \text{cm}$  pitch. Thicker shield wires were placed between the sense wires to ensure the avalanches remained localised.

The electric field in the drift volume was nominally uniform with strength  $16\ \text{V}/\text{mm}$ . However the field is non-uniform by up to  $10\%$  due to the field at the sense planes leaking into the drift volume, and by  $\sim 1\%$  due to modular interference[30]. Ultimately the non-uniformity in the electric field is addressed by iterating the STRs using real tracks.

---

<sup>15</sup>This gas was chosen since it was already in use in the drift chambers. See Section 3.8 for the advantages of Dimethylether.

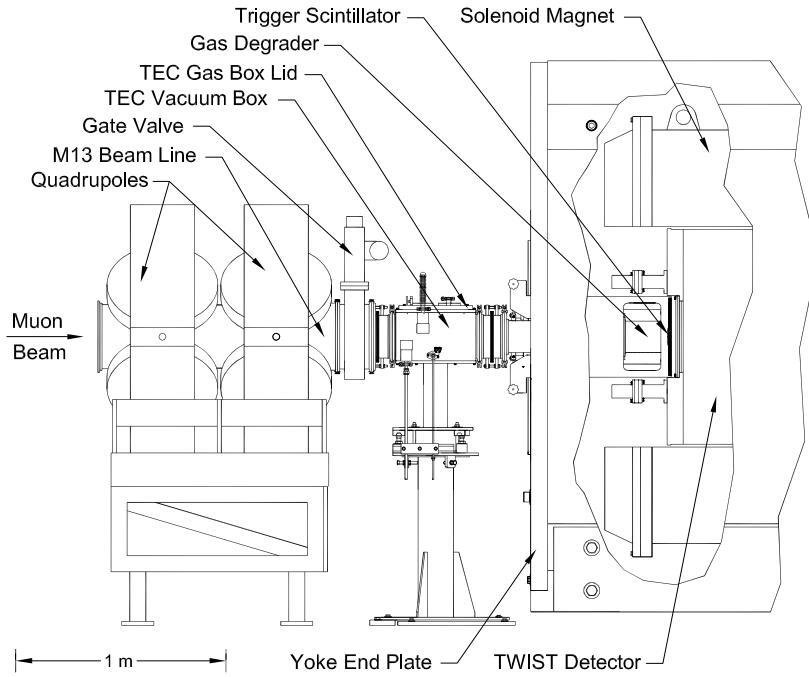


Figure 3.5: The positioning of the time expansion chambers relative to the M13 beam line and solenoid. This is Fig. 1 from Ref. [30].

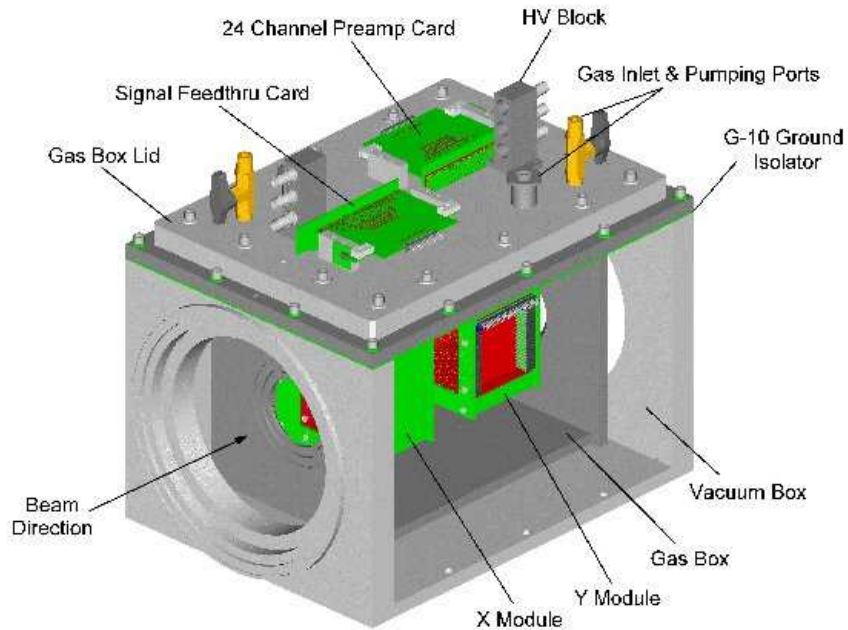
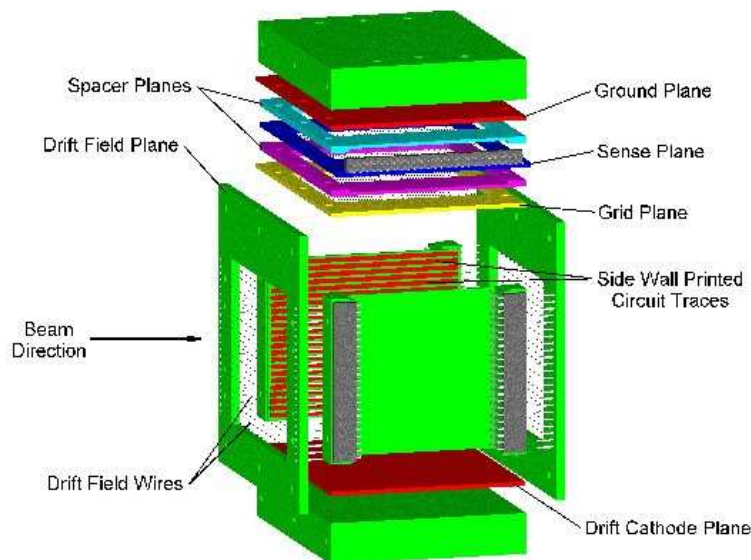
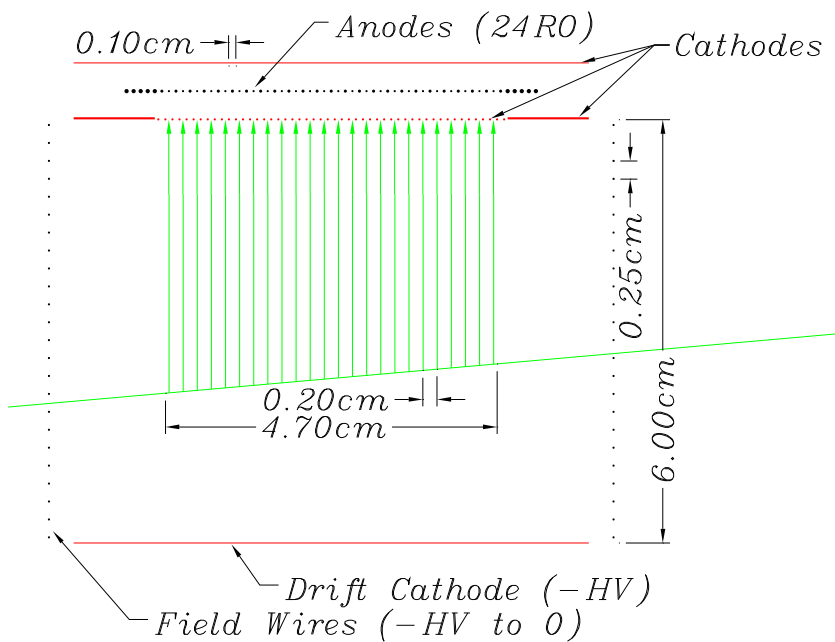


Figure 3.6: The location of the time expansion chamber modules and their electronics is shown. This is Fig. 2 from Ref. [30].



(a) Components of a single time expansion module. This is Fig. 3 from Ref. [30].



(b) Cross section through a single time expansion module, with dimensions shown. The initial ionisation is indicated by the green line through the entire module. The green arrows show the direction of the drift electrons. This is Fig. 2.13 from Ref. [36].

Figure 3.7: An individual time expansion chamber module.

### 3.16 Calibration of time expansion chambers

The sense planes in the time expansion chambers required the following calibrations: space-time relationship (STR) for each drift cell, wire time offsets for individual wires, global time offset with respect to detector trigger and discriminator amplitude walk. The technique for each will now be summarised.

The STR for each cell was initially generated using the GARFIELD software[45]<sup>29</sup>. The STR for each cell was then corrected using real tracks, since this properly accounts for the interference in electric field between the  $x$  and  $y$  module, as well as voltage and geometry differences from the GARFIELD inputs. Two collimators with 121 holes were placed on each end of the box containing the TECs, as shown in Fig. 3.26(a). This design is an improvement over the published method[30], which described a 49 hole collimator, and the previous  $P_\mu^\pi \xi$  analysis, which used a four hole collimator[36]. The beam line was tuned to provide a spread muon beam, and low angle tracks were selected. The STRs were adjusted to place the collimator holes at their known positions; Fig. 3.26(b) shows an example of the calibration data after the STRs have been determined.

The relative wire time offsets were determined by selecting tracks from the centre hole of the collimator, and histogramming the times for each wire. The offset required to match the peaks of the histograms was then determined. A global time offset relative to muon scintillator was then determined from the difference in the times between the peak of the wire histograms and the scintillator signal.

The concept of discriminator amplitude walk is shown in Fig. 3.27. The calibration determines the linear relationship between rising edge time and pulse width.

In practice, the relative and global wire time offsets were determined first, followed by the discriminator amplitude walk. The process was then iterated until convergence. The STRs were determined last, also in an iterative procedure.

An engineering run in 2005 found the sense planes became less efficient after several hours of use. For 2006 and 2007 the sense planes were therefore regularly changed. There are other concerns related to the calibration that are reserved for Chapter 5, such as comparisons of the four independent calibrations from 2006/7, the temperature dependence of the STRs, efficiency that depends on distance from the sense plane, and more detailed studies of sense plane aging. The STRs have confirmed to be the same with the magnetic field on and off[30].

---

<sup>29</sup>GARFIELD has been widely used to simulate drift cell response since 1984, and is still actively supported.

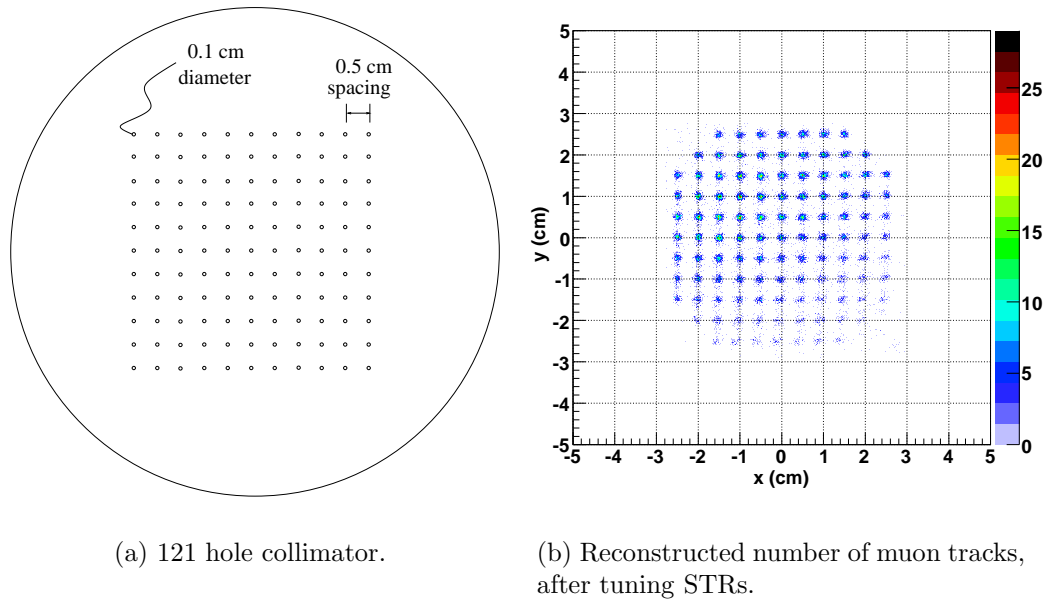


Figure 3.26: Apparatus to determine TEC drift cell space-time relationships (STRs).

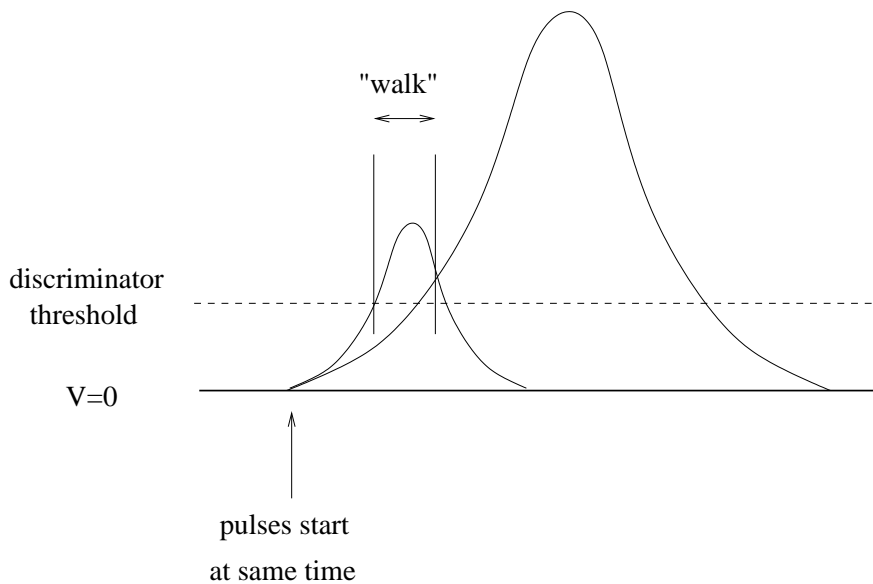


Figure 3.27: Discriminator amplitude walk. Two pulses that start at the same time but have different pulse heights will have different leading edge times.